Accepted Manuscript

Title: A one-dimensional dynamic analysis of strain-gradient viscoplasticity

Authors: An Danh Nguyen, Marcus Stoel, Dieter Weichert

PII: S0997-7538(10)00095-1

DOI: 10.1016/j.euromechsol.2010.07.004

Reference: EJMSOL 2630

To appear in: *European Journal of Mechanics / A Solids*

Received Date: 16 April 2010

Revised Date: 8 June 2010

Accepted Date: 13 July 2010

Please cite this article as: Nguyen, A.D., Stoel, M., Weichert, D. A one-dimensional dynamic analysis of strain-gradient viscoplasticity, European Journal of Mechanics / A Solids (2010), doi: 10.1016/j.euromechsol.2010.07.004

A one-dimensional dynamic analysis of strain-gradient viscoplasticity

An Danh Nguyen, Marcus Stoffel, and Dieter Weichert

Institute of General Mechanics, Templergraben 64, 52056 Aachen, Germany

Abstract Based on the static theory of strain-gradient viscoplasticity proposed by Anand et al. (2005), a one-dimensional dynamic analysis is derived for finite element computation of isotropic hardening materials. The kinetic energy is assumed to be composed of the conventional and internal kinetic energy. The internal energy is described phenomenologically in terms of the equivalent plastic strain in order to capture the heterogeneity of plastic flow. Herein the microscopic density is assumed to be related to the macroscopic one through a microscopic-inertia parameter. The macroscopic-force balance and microscopic-force balance including inertia effects are derived. The performance of the proposed formulation is illustrated through the numerical simulation of a one-dimensional dynamic problem. A parameter study to find the microscopic-inertia parameter is carried out. At last, suitable microscopic boundary conditions and dynamic effects are discussed through comparison with the conventional plasticity.

1 Introduction

It is well-known that the continuum formulation of strain localization in materials by using the conventional plasticity theory leads to the ill-posedness of the boundary value problem (BVP) and, consequently, mesh-dependence, incorrect size effect, and excessive damage localization. The ill-posedness of BVP is characterized by the loss of ellipticity in statics and of hyperbolicity in dynamics when materials soften. In dynamics, the differential equations of motion become ill-posed as the wave velocity becomes imaginary (Luzio(2005)). A possibility to overcome such the mathematical difficulty is to introduce the gradient of plastic strain or the damage parameter fields in order to penalize possible sharp localization Q.S. Nguyen (2005). The use of gradients in the localization of deformation and fracture allows to obtain the thickness of shear band and to simulate the effect of surface tension forces (Aifantis (1992)). An additional advantage of this treament is that the heterogeneity of plastic flow in microscopic scales can be captured. For this reason, the strain-gradient theory is used in the presented dynamical analysis.

In the last years much research has been devoted to strain gradient plasticity theories and different strain gradient plasticity models have been proposed by many authors such as e.g. Aifantis (1984,1987), Mühlhaus and Aifantis (1991), Fleck (1993) and Hutchinson (2001), Fleck et al. (1994), de Borst et al. (1992, 1996, 1999), Zbib (1989). We can also find the development of the Cosserat strain gradient theory proposed by Forest et al. (2003). In most of these models, the yield stress is assumed to depend on gradients of plastic strain.

Constitutive equations by incorporating high-order gradients are used to describe length scale effects. Consequently, additional boundary conditions must be presented. Numerical strategies for the treatment of gradient plasticity at small strains were investigated by Sluys (1995), de Borst and Mühlhaus (1992) and Pamin (1994). Similarly, gradient damage theories for isotropic and anisotropic damage can be found in literature, i.e. Peerlings (1998), Voyiadjis (2004). Gudmundson (2004) reported the unified treatment which is able to cover a large range of strain gradient plasticity effects in isotropic materials (Gudmundson (2004)). Both incremental plasticity and viscoplasticity models are presented in his work. Gurtin (2000, 2002) developed large deformation strain gradient viscoplasticity in single crystals. The theory is based on classical crystalline kinematics; microscopic forces for each slip system consistent with a microscopic force balance; a mechanical version of the second law of thermodynamics that includes, via the microscopic forces, work performed during slip; a rate-independent constitutive theory including gradient of plastic strains and plastic strain rates. With such the constitutive theory, the free energy depends on the gradient of plastic strains and strain hardening depends on the plastic strain and a scalar measure to the accumulation of geometrically necessary dislocation as well as a dissipative part of a vector microstress to depend on the gradient of the plastic strain rate. Based on Gurtin's work, Anand et al. (2005), Lele and Anand (2008a, 2008b, 2009) developed the strain gradient theory for isotropic viscoplastic materials for small and large deformations.

In dynamic analysis, a good insight into strain localization can be gained from the analysis of wave propagation by using strain gradient or nonlocal theories. Sluys et al. (1992,1995) and de Borst et al. (1995) investigated wave propagation and dispersion for a gradient plasticity model. Peerlings et al. (1996) have shown that in a one-dimensional setting the hyperbolicity of the governing equations is preserved in the softening regime for strain gradient models. The regularisation techniques of nonlocal or by gradient approaches for damage models were developed by many authors, i.e. Peerlings et al. (1996, 1998, 2001), Askes et al.(2000, 2002a, 2002b), Luzio and Bazant (2005). An analytical solution of dynamic behaviour for a micro beam is reported in Kong et al. (2009).

Among the strain-gradient theories mentioned above, the static approaches developed by Gurtin (2000, 2002, 2003), Anand (2005) and Lele (2008a, 2008b, 2009) are particularly interesting for our study since they can be extended easily to dynamic analysis with integrating strain-gradient viscoplasticity law. Therefore, as the first attempt, this paper presents a one-dimensional dynamic analysis based on the static theory of strain-gradient plasticity proposed by Anand et al. (2005), Lele (2008a). We will establish the equation of motion and variational formulation for finite element computation of isotropic hardening materials. Although the presented analysis can be applied for softening materials, it should be noted that such effects are not investigated numerically in this paper. The performance of the proposed formulation is then illustrated through several numerical examples. Dynamic effects such as microscopic inertia effects, artificial damping are discussed. Besides, we investigated the effects of hard boundary conditions proposed by Anand (2005) for the

dynamic cases to find out more suitable boundary conditions such that the obtained results without length scales are close to that of the conventional plasticity.

In this study, the kinetic energy is assumed to be composed of the conventional energy and micro-kinetic one. The latter one is assumed to be a function of the plastic shear strain to take into account the effects of micro-inertia in zones of strain localzation. The microscopic density is assumed to be related to the macroscopic density through a microscopic-inertia parameter. In this paper, first, the macroscopic-force balance and microscopic-force balance including inertia effects are derived. Then, a finite element formulation for the one-dimensional dynamic analysis is presented. Next, numerical results are presented and compared to the results of classical dynamic problems obtained by ABAQUS. Finally, a parameter study to find the microscopic-inertia parameter is carried out.

2 Governing equations

We consider a strip B of finite width $(0 \leq y \leq h)$ dynamically loaded by a dynamic simple shear with shear stress τ. Based on the static theory of strain-gradient viscoplasticity proposed by Anand (2005) and Lele (2008a)'s work, in this section, first we derive a variational formulation for the dynamic analysis. Then, the principle of virtual power is introduced taking into account inertia and body forces in order to obtain the macroscopic- and microsopic-force balances.

A one-dimentional model in Figure 1 is used to simulate the strip. We consider $P = [y_1, y_2]$ as a part of $B = [0, h]$, and recall the following notation for a field Φ as written by Anand (2005) and Lele (2008a)

$$\int_P \Phi dy = \int_{y_1}^{y_2} \Phi dy, \quad [\Phi]_{\partial P} = \Phi(y_2) - \Phi(y_1)$$

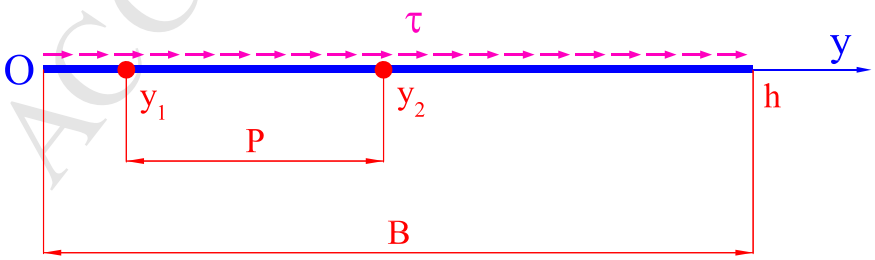

Figure1. A one-dimensional model

In the sequel, a superimposed dot denotes time derivative, a lower-index derivative with respect to the coordinate following a comma. Adopting the standard kinematical

assumption of the shear strain $\gamma(y,t) = \frac{\partial u(y,t)}{\partial y}$, and a decomposition of shear strain into the elastic strain γ^e and the plastic strain γ^p, i.e. $\gamma(y,t) = \gamma^e(y,t) + \gamma^p(y,t)$, the uniaxial velocity of a material point $\dot{u}$, the elastic strain rate $\dot{\gamma}^e$ and the plastic strain rate $\dot{\gamma}^p$ are expressed by

$$\dot{u}_{,y} = \dot{\gamma}^e + \dot{\gamma}^p \tag{1}$$

To capture the heterogeneity of plastic flow in the static case, Mülhaus (1991) and Aifantis (1992) modified the classical theory of rate-independent plasticity by incorporating higher-order gradients of the equivalent plastic strain γ^p into the yield condition. A complete balance for the yield stress, which is assumed to depend on the equivalent plastic strain γ^p alone, contains a diffusive-like term in the evolution of the back stress. It is pointed out that the second time derivatives of the back stress or of the equivalent plastic strain can appear in the evolution law. Using the strain-gradient theory proposed by Anand et al. (Anand (2005) and Lele (2008a)), the BVP for the dynamical problem now can be introduced as follows

$$\tau_{,y} + b - \kappa\dot{u} = \rho\ddot{u} \tag{2}$$

$$k^p_{,y} - \tau^p + \tau - \kappa^p\dot{\gamma}^p = \rho^p\ddot{\gamma}^p \tag{3}$$

with regarding the boundary conditions as in Lele's work, which are recalled here

- macroscopic boundary conditions: $\tau(0,t) = \tau(h,t) = \tau^*(t)$; $u(0,t) = 0$, $u(h,t) = u^*(t)$
- microscopic boundary conditions, which are restricted to microscopically hard boundary-conditions: $\dot{\gamma}^p(0,t) = \dot{\gamma}^p(h,t) = 0$ and null initial-condition $\gamma^p(y,0) = 0$

Here τ^p, k^p, b, ρ, ρ^p, κ, and κ^p denote respectively microscopic stress, gradient of microscopic stress, body force, mass density, plastic inertia density, damping factor, plastic damping factor. Due to the appearance of γ^p as an additional degree of freedom, its boundary condition has to be introduced.

The dynamical terms $\rho^p\ddot{\gamma}^p$, $\kappa^p\dot{\gamma}^p$ are assumed to measure the microscopic inertia and dissipation respectively. For the microscopic inertia, the inertia term ρ^p is assumed to be related to the macroscopic one by

$$\rho^p = I_\rho\rho \tag{4}$$

where I_ρ is a microscopic inertia factor with the dimension of mass per length.

Similarly, for microscopic damping, κ^p is assumed in the form

$$\kappa^p = I_\kappa\kappa \tag{5}$$

where I_κ is a microscopic damping factor with the dimension of force multiplied by time.

For two arbitrary fields $\tilde{u}$ and $\tilde{\gamma}^p$, the weak form of equilibrium of macroscopic and microscopic forces is defined by

$$\int_P \left(\tau_{,y} + b - \kappa\dot{u} - \rho\ddot{u}\right)\tilde{u}\ dy = 0 \tag{6}$$

$$\int_P \left(k^p_{,y} - \tau^p + \tau - \kappa^p\dot{\gamma}^p - \rho^p\ddot{\gamma}^p\right)\tilde{\gamma}^p\ dy = 0 \tag{7}$$

With the use of the integration by parts and divergence theorem, the first term in (6) reads

$$\int_P \tau_{,y}\tilde{u}dy = -\int_P \tau\tilde{u}_{,y}dy + [\hat{\tau}\tilde{u}]_{\partial P} \tag{8}$$

with $\tau = \hat{\tau}$ on the boundary of P, denoted as ∂P, where $\hat{\tau}$ denotes macroscopic traction.

Similarly, the first term of the integral (7) becomes

$$\int_P k^p_{,y}\tilde{\gamma}^p dy = -\int_P \tilde{\gamma}^p_{,y}k^p dy + \left[\hat{k}^p\tilde{\gamma}^p\right]_{\partial P} \tag{9}$$

with $k^p = \hat{k}^p$ on the boundary ∂P, where $\hat{k}^p$ denotes microscopic traction.

Substitution of (8) and (9) into (6), (7) respectively, yields

$$-\int_P \tau\tilde{u}_{,y}dy + [\hat{\tau}\tilde{u}]_{\partial P} + \int_P b\tilde{u}dy - \int_P \kappa\dot{u}\tilde{u}dy - \int_P \rho\ddot{u}\tilde{u}dy = 0 \tag{10}$$

$$-\int_P \tilde{\gamma}^p_{,y}k^p dy + \left[\hat{k}^p\tilde{\gamma}^p\right]_{\partial P} - \int_P \tau^p\tilde{\gamma}^p dy + \int_P \tau\tilde{\gamma}^p dy - \int_P \kappa^p\dot{\gamma}_p\tilde{\gamma}^p dy - \int_P \rho^p\ddot{\gamma}^p\tilde{\gamma}^p dy = 0 \tag{11}$$

The integral identities (10) and (11) express the respective field equations in the global (integral) form and provide the variational basis for the finite element formulations of the problem.

By summing up (10) with (11) and taking into account (1), the principle of virtual power can be obtained

$$-W_{int} + W_{kin} + W_{ext} = 0 \tag{12}$$

where W_{ext}, W_{int} and W_{kin} denote the external, internal, and kinetic virtual power, which are defined by

$$W_{ext} = \left[\hat{\tau}\tilde{u} + \hat{k}^p\tilde{\gamma}^p\right]_{\partial P} + \int_P b\tilde{u}dy \tag{13}$$

$$W_{int} = \int_P \left(\tau\tilde{\gamma}^e + \tau^p\tilde{\gamma}^p + k^p\tilde{\gamma}^p_{,y}\right)dy + \int_P \kappa\dot{u}\tilde{u}dy + \int_P \kappa^p\dot{\gamma}_p\tilde{\gamma}^p dy \tag{14}$$

$$W_{kin} = \int_P \rho\ddot{u}\tilde{u}\ dy + \int_P \rho^p\ddot{\gamma}^p\tilde{\gamma}^p dy \tag{15}$$

where $\tilde{u}$, $\tilde{\gamma}^e$, and $\tilde{\gamma}^p$ denote virtual velocities of displacement, elastic shear strain, and plastic shear strain respectively.

3 Finite element formulation

The macroscopic and microscopic virtual power relations (10) and (11) are rewritten here

$$\int_P \rho\ddot{u}\tilde{u}\ dy + \int_P \kappa\dot{u}\tilde{u}dy + \int_P \tau\tilde{u}_{,y}dy - \int_P b\tilde{u}dy - [\hat{\tau}\tilde{u}]_{\partial P} = 0 \tag{16}$$

$$\int_P \rho^p\ddot{\gamma}^p\tilde{\gamma}^p dy + \int_P \kappa^p\dot{\gamma}_p\tilde{\gamma}^p dy + \int_P \left\{(\tau^p - \tau)\,\tilde{\gamma}^p + \tilde{\gamma}^p_{,y}k^p\right\} dy - \left[\hat{k}^p\tilde{\gamma}^p\right]_{\partial P} = 0 \tag{17}$$

with the boundary conditions as mentioned above.

The constitutive laws proposed by Anand (2005), which take into account viscoplastic behavior and characterize internal hardening or softening, are adopted. The constitutive theory depends on gradients of both plastic shear strain $\gamma^p_{,y}$ and plastic shear strain rate $\dot{\gamma}^p_{,y}$. Microscopic stress τ^p takes a similar form of the conventional plasticity, while gradient k^p of the microscopic stress admits a decomposition into energetic and dissipative parts, which are adjusted by length scale parameters L, l. The effective flow rate d^p is generalized to include a dependence on $\left|\dot{\gamma}^p_{,y}\right|$. A summary of the constitutive laws is given below.

$$\tau = \mu\left(u_{,y} - \gamma^p\right) \tag{18}$$

$$\tau^p = S\left(\frac{d^p}{d_0}\right)^m \frac{\dot{\gamma}^p}{d^p} \tag{19}$$

$$k^p = S_0 L^2\gamma^p_{,y} + S_0 l^2\left(\frac{d^p}{d_0}\right)^m \frac{\dot{\gamma}^p_{,y}}{d^p} \tag{20}$$

$$\dot{S} = H\left(S\right)d^p, \quad S\left(y,0\right) = S_0 > 0 \tag{21}$$

$$d^p = \sqrt{\left|\dot{\gamma}^p\right|^2 + l^2\left|\dot{\gamma}^p_{,y}\right|^2} \tag{22}$$

where d^p, L, l denote respectively equivalent plastic strain rate, energetic length scale and dissipative length scale; S, S_0, $H(S)$, d_0, d_p and m denote respectively the current resistance to plastic flow, shear yield strength, hardening (or softening) function, reference flow rate, effective flow rate, rate-sensitive parameter.

Let us denote $\boldsymbol{U} = \left[u, \quad \gamma^p\right]^T$, $\dot{\boldsymbol{U}} = \left[\dot{u}, \quad \dot{\gamma}^p\right]^T$, $\ddot{\boldsymbol{U}} = \left[\ddot{u}, \quad \ddot{\gamma}^p\right]^T$. After discretization, the above governing equations (16-17) can be written in matrix form as

$$\boldsymbol{M}\ddot{\boldsymbol{U}} + \boldsymbol{I} - \boldsymbol{P} = 0 \tag{23}$$

where the consistent mass matrix $\boldsymbol{M}$ reads

$$\boldsymbol{M} = \begin{bmatrix} \int_B \rho\boldsymbol{N}^T\boldsymbol{N}dy & \boldsymbol{0} \\ \boldsymbol{0} & \int_B \rho^p\boldsymbol{N}^T\boldsymbol{N}dy \end{bmatrix} \tag{24}$$

The internal force vector $\boldsymbol{I}$ is defined by

$$\boldsymbol{I} = \boldsymbol{K}\boldsymbol{U} + \boldsymbol{C}\dot{\boldsymbol{U}} \tag{25}$$

where $\boldsymbol{K}$ is a global stiffness which is formed by assembly of element stiffness matrix, which is described in details in Anand (2005) and Lele (2008a)'s work

$$\boldsymbol{K}^e = \begin{bmatrix} \boldsymbol{K}^e_{uu} & \boldsymbol{K}^e_{u\gamma^p} \\ \boldsymbol{K}^e_{\gamma^p u} & \boldsymbol{K}^e_{\gamma^p\gamma^p} \end{bmatrix} \tag{26}$$

and damping matrix reads

$$\boldsymbol{C} = \begin{bmatrix} \int_B \kappa \boldsymbol{N}^T \boldsymbol{N} dy & \mathbf{0} \\ \mathbf{0} & \int_B \kappa^p \boldsymbol{N}^T \boldsymbol{N} dy \end{bmatrix} \tag{27}$$

With the absence of the macroscopic and microscopic tractions in this study, the external force vector $\boldsymbol{P}$ is determined by

$$\boldsymbol{P} = \begin{bmatrix} \int_B f_{body} \boldsymbol{N}^T dy \\ \mathbf{0} \end{bmatrix} \tag{28}$$

The initial value problem for (23) consists of finding a function $\boldsymbol{U} = \boldsymbol{U}(t), t \in [0, T],\ T > 0$, satisfying the initial conditions

$$\boldsymbol{U}_0 = \bar{\boldsymbol{U}} \tag{29}$$

$$\dot{\boldsymbol{U}}_0 = \dot{\bar{\boldsymbol{U}}} \tag{30}$$

Hilber-Hughes-Taylor's time integration scheme (ABAQUS, Hilber (1977), Hilber(1978)) is used to obtain the approximate solutions by one step difference method (see Appendix).

4 Numerical examples and discussions

The presented finite element formulation for dynamic analysis using the strain-gradient viscoplasticity is implemented in the user element subroutine compiled with ABAQUS. One-dimensional simulations are carried out to investigate the dynamic response. For these simulations, a rod in Figure 2 depicts schematically the strip B with a unity width and is discretized with a mesh of 15 elements in finite element computation. The following material parameters are used to produce the numerical results shown below

- Elastic shear modulus $\mu = 100 \times 10^9 Pa$;
- Initial yield limit $S_0 = 100 \times 10^6 Pa$;
- Reference strain-rate $d_0 = 0.1$;
- Strain-rate sensitive parameter $m = 0.02$.

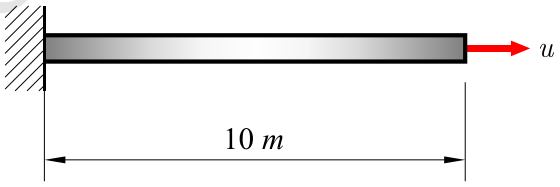

Figure2. Scheme of a rod subjected to prescribed displacement

Further, the material behaviour is assumed to be linear isotropic hardening, i.e.

$$H(S) = H_0 = constant \tag{31}$$

Most of the numerical results are compared with that of quasi-static loading and are presented in the following sections. The obtained results coincide with the quasi-static one.

4.1 Case 1: Perfectly plasticity ($L = 0.0m$; $l = 0.0m$) - Triangular loading

First, we investigated the structure subjected to the triangular loading of prescribed displacements as shown in Figure 3 with material behavior assumed to be perfectly plastic for verification purpose. Neither energetic-gradient nor dissipative-gradient hardening is taken into account in this case. The following input material parameters are used $\rho = 7800kg/m^3$; $b = 78000kg/m^3 \times m/s^2$; $\kappa = 0.0Ns/m$. Figures 4 and 5 show average strain and stress curves $\Gamma - \tau$ and history of plastic strain γ^p at the Gaussian point of the coordinate of $y = 9.925m$ for cases of $I_\rho = 10.0, 1.0, 0.5, 0.1\frac{kg}{m}$. Here, the average strain Γ is defined by the ratio between displacement u and the whole length h of the rod, i.e. $\Gamma = \frac{u}{h}$.

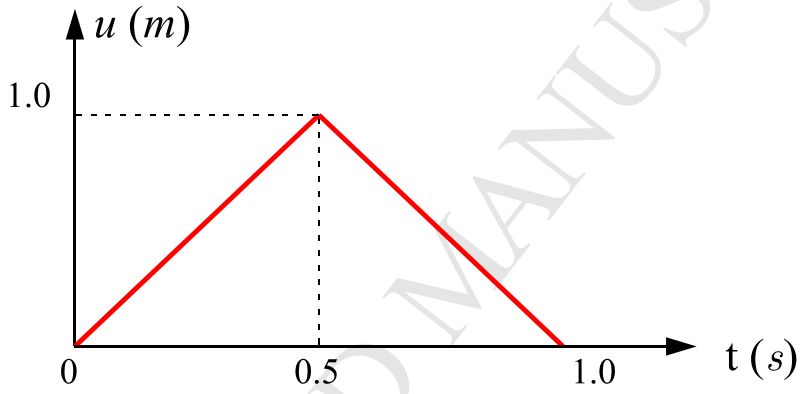

Figure3. Prescribed displacements as triangular impulse loading

It is observed that as expected the presented results match well the result with using the conventional plasticity theory in ABAQUS Standard module. There is a small gap between two distributions of shear stresses due the microscopically hard boundary conditions of the plastic strain rates $\dot{\gamma}^p = 0$ at both ends of the rod. The vibrations, which appear at the beginning and over the peak of loading, are dissipated quickly. This may be explained by microscopic inertia effects, which are described by I_ρ factor and plastic shear strain γ^p, and by expense of a loss of accuracy due to the numerical time integration scheme. The expense of the loss of accuracy introduced artificial damping in dynamic effects and a difference of Γ in comparison with quasi-static case. The fast decrease of vibration is observed and in case of $I_\rho = 0.5$ the response is close to that obtained by the conventional theory.

In despite of the two different forms of partial derivative equations with different boundary conditions, the two models can be comparable because the strain-gradient plasticity is a generalization of conventional plasticity. Therefore, it is reasonable to calibrate the microscopic inertia factor I_ρ based on the conventional plastic model such that the unique physical phenomena can be simulated, especially in cases without length scales and microscopic inertia factor I_ρ.

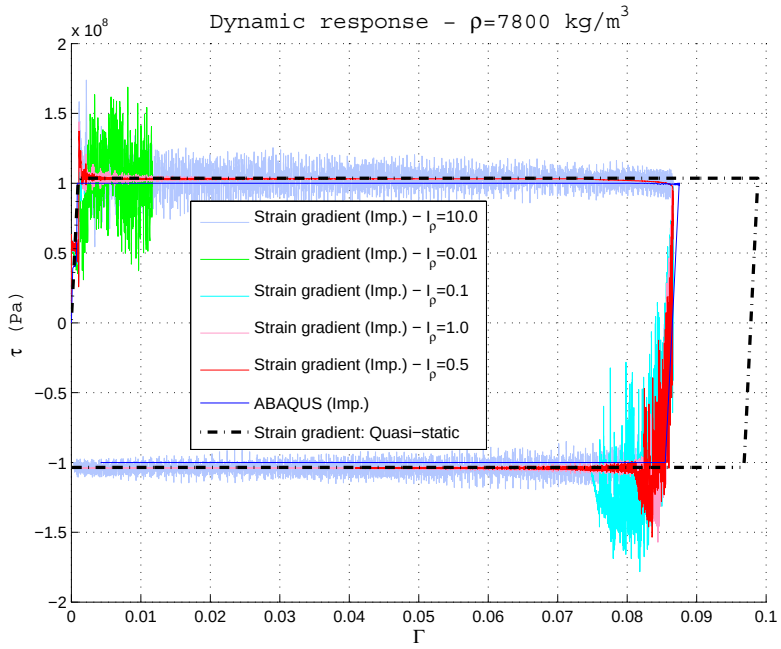

Figure4. Case 1 - Dynamic response $\Gamma - \tau$ at $y = 9.925m$

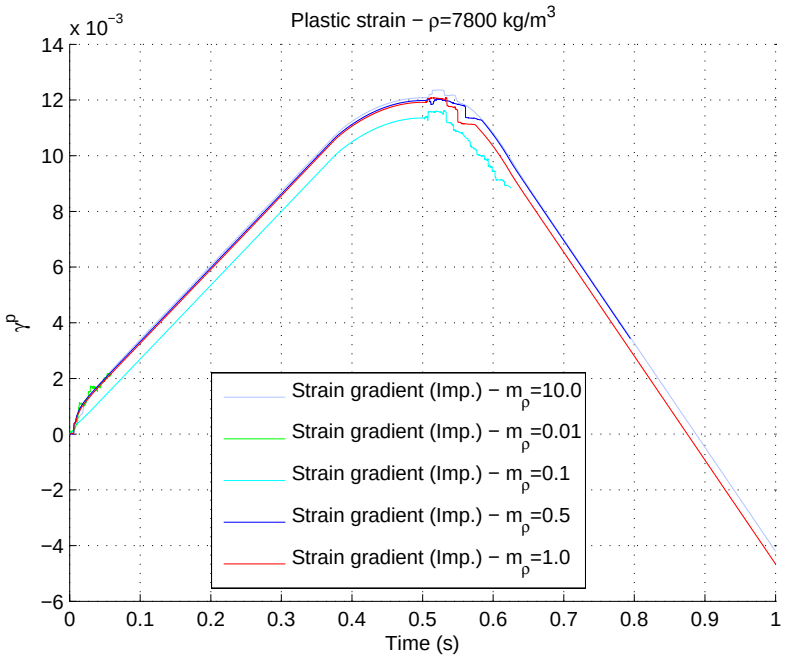

Figure5. Case 1 - Shear plastic strains γ^p at $y = 9.925m$

4.2 Case 2: Perfect plasticity ($L = 0.0m$; $l = 0.0m$) - Sinusoidal loading

The previous example is solved again for the case of sinusoidal loading as shown in Figure 6. From parameter study of the microsopic inertia factor, the best value of I_ρ is found to

be 0.25. The presented results shown in Figures 7, 8 match well that of the conventional theory obtained by ABAQUS Standard module. The observations of dynamic effects are similar to that of the above example except that the expense of a loss of accuracy due to the numerical time integration scheme decreases.

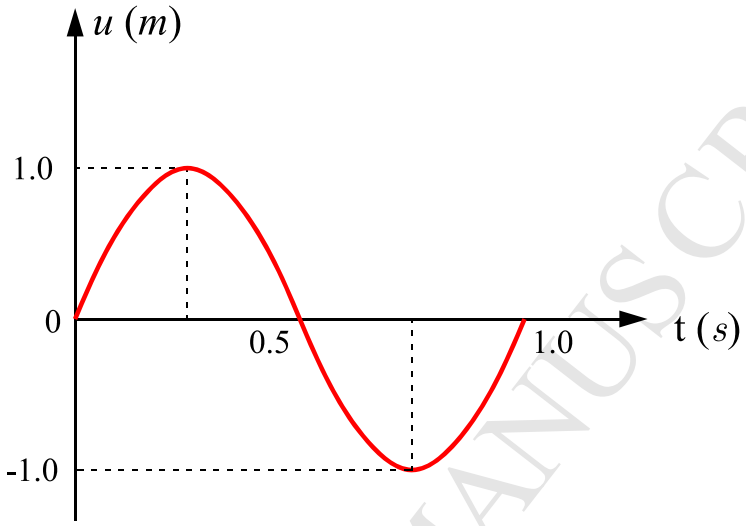

Figure6. Sinusoid loading of displacements

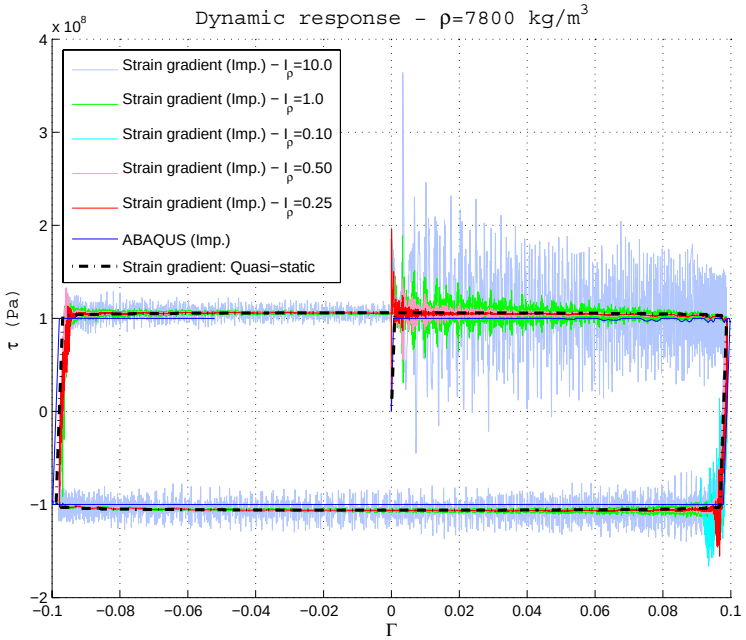

Figure7. Case 2 - Dynamic response $\Gamma - \tau$ at $y = 9.925m$

The distributions of shear plastic strain γ^p along the length of the rod are shown in Figure 8. Here, it should be noted that due to the microscopically hard boundary conditions the rates of plastic strain $\dot{\gamma}^p = 0$ at both ends of the rod are equal to zero. The distribution of γ^p is not a monotonic distribution as we obtained by using the conventional theory. An investigation of mesh sensitivity is given in Figure 10. Except the regions near both ends of the rod, the distributions of plastic strain are nearly unchanged.

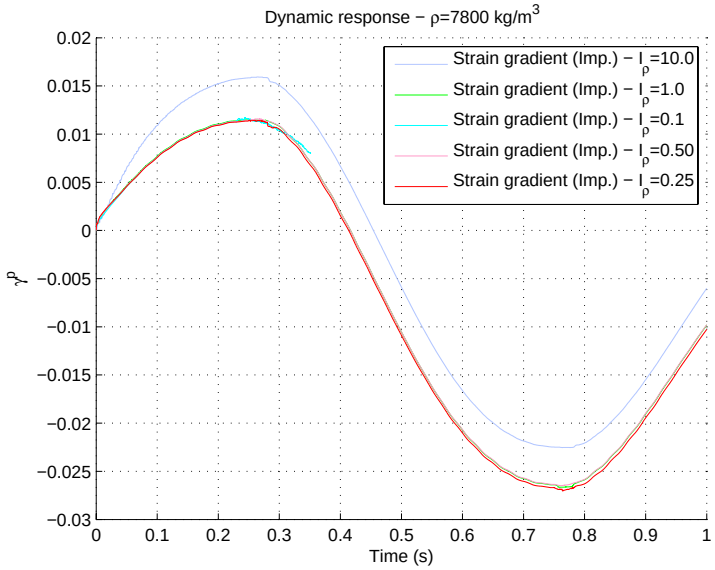

Figure8. Case 2 - Shear plastic strains γ^p at $y = 9.925m$

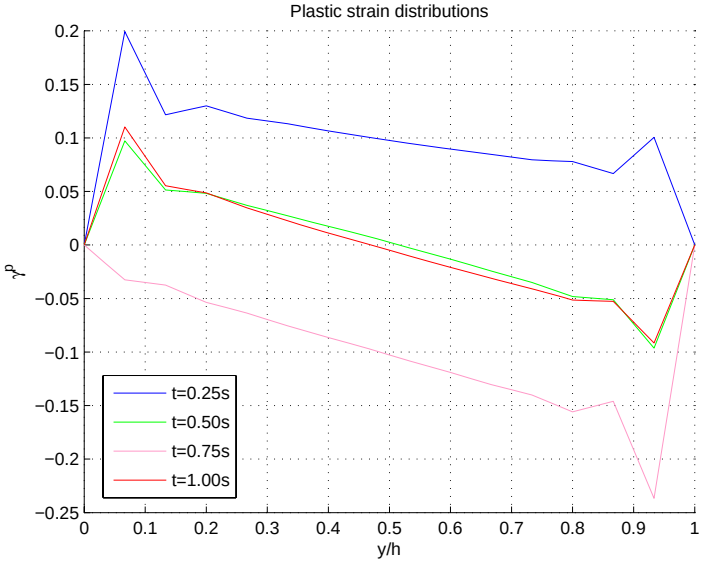

Figure9. Case 2 - Distribution of shear plastic strain γ^p, $I_\rho = 0.25\frac{kg}{m}$

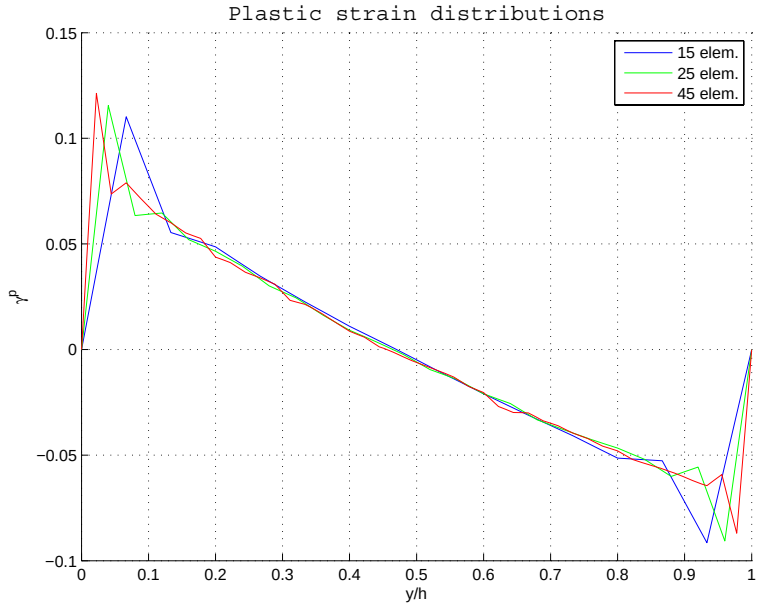

Figure10. Case 2 - Mesh sensitivity on distribution of shear plastic strain γ^p, $I_\rho = 0.25\frac{kg}{m}$, $t = 1.0s$

4.3 Case 3: Isotropic hardening without length scales ($L = 0.0m$; $l = 0.0m$) - Sinusoidal loading

The problem is also investigated with assumption of isotropic hardening behavior of material without length scale effects ($L = 0.0m$; $l = 0.0m$). The presented numerical results shown in Figures 11, 12 are compared with the case that the material is assumed to be linear isotropic hardening in the conventional plasticity theory. Here, we assume $\frac{d^p}{d_0} \approx 1$ to find the hardening parameters for the mechanical computation using the conventional theory. The best value of I_ρ is found to be $0.25\frac{kg}{m}$. The response $\Gamma - \tau$ obtained in the case $I_\rho = 0.25\frac{kg}{m}$ is close to that of ABAQUS result. The distributions of shear plastic strain γ^p along the length of the rod are depicted in Figures 13, 14 for the case using the presented gradient theory with $I_\rho = 0.25\frac{kg}{m}$ and the one using the conventional plasticity theory, respectively. Again we can observe the effect of the microscopic boundary condition on the presented distribution of τ as well as γ^p.

4.4 Case 4: Energetic-gradient hardening - Sinusoidal loading

We also investigated the case of energetic-gradient hardening with the length scale parameters of $L = 10.0m$ and $l = 0.0m$. The presented dynamic effects are depicted in Figures 15, 16. The best value of I_ρ is also $0.25\frac{kg}{m}$ for this case. The strain-hardening rate and Bauschinger-effect give arise as the energetic-gradient hardening L is different to zero. Unlike in case 3, the distribution of γ^p shown in Figure 17 is smooth and has the maximum value at the midddle of the rod.

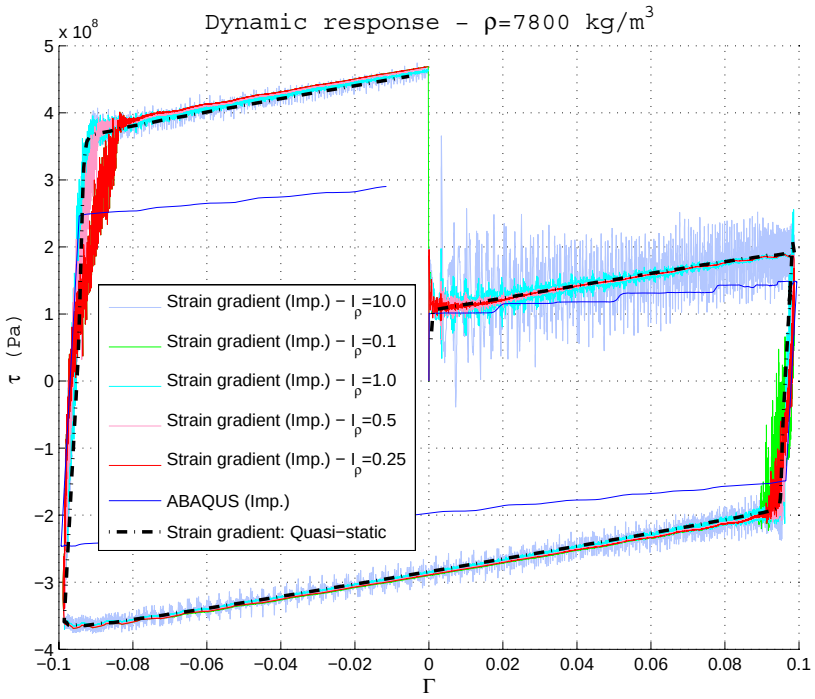

Figure11. Case 3 - Dynamic response $\Gamma - \tau$ at $y = 9.925m$

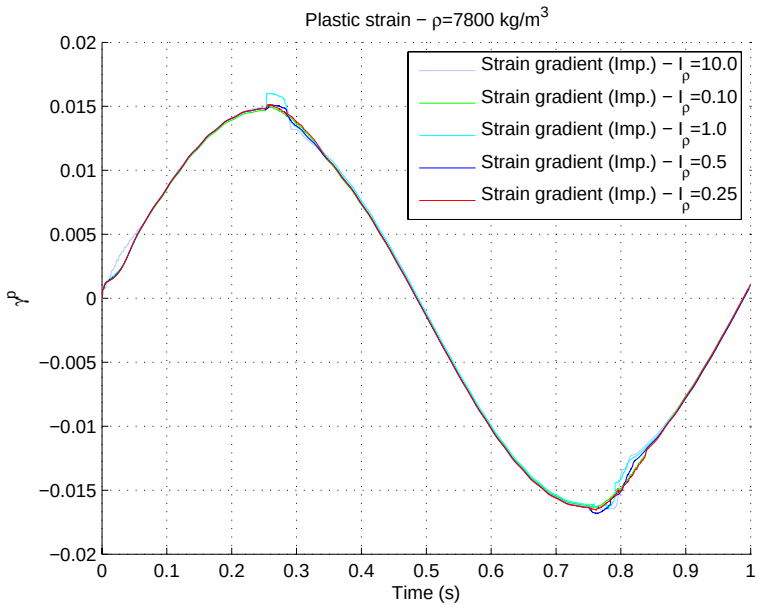

Figure12. Case 3 - Shear plastic strain γ^p at $y = 9.925m$

4.5 Case 5: Null initial-conditions of equivalent plastic strains $\boldsymbol{\gamma^p(0,0) = 0}$ and $\boldsymbol{\gamma^p(h,0) = 0}$

The case 3 is solved again to investigate an effect of boundary conditions on the dynamic reponse. The microscopic boundary conditions in section 2 is modified such that no internal

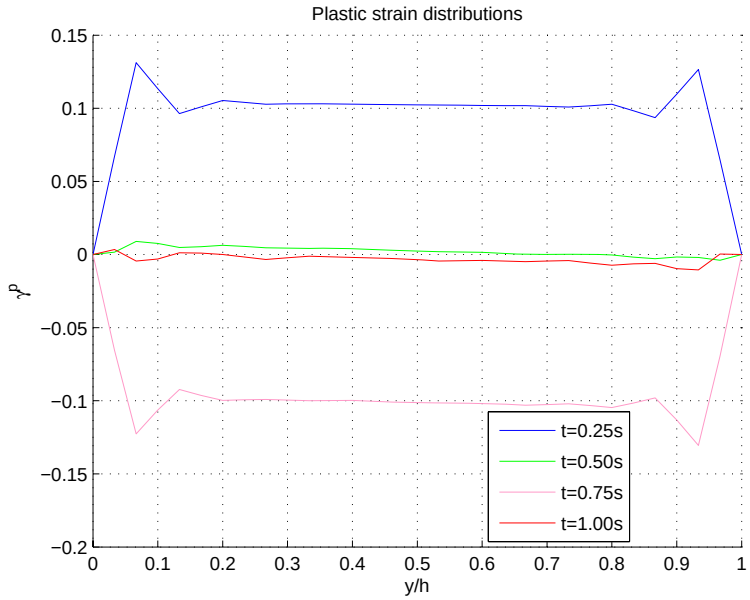

Figure13. Case 3 - Distribution of shear plastic strain γ^p, $I_\rho = 0.25\frac{kg}{m}$

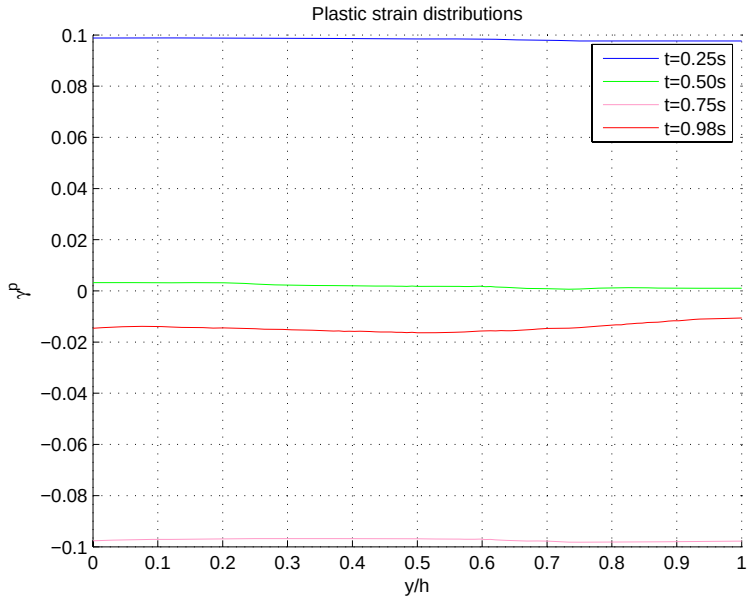

Figure14. Case 3 - Distributions of shear plastic strain $\gamma^p\,(x,t)$ (Conventional plasticity theory)

expenditure of power exists at the initial instant of loading. This has the consequence that the equivalent plastic strain at the free ends of the rod are null, i.e. $\gamma^p(0,0) = 0$ and $\gamma^p(h,0) = 0$. The best value I_ρ of $0.25\frac{kg}{m}$ is used for this investigation. In Figure 18, the obtained dynamical response $\Gamma - \tau$ is close to that of ABAQUS result. The distributions

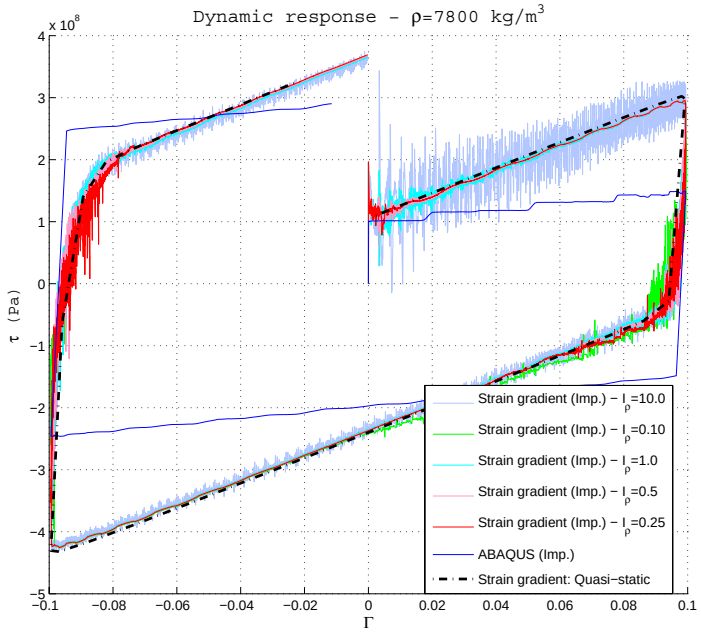

Figure15. Case 4 - Dynamic response $\Gamma - \tau$ at $y = 9.925m$

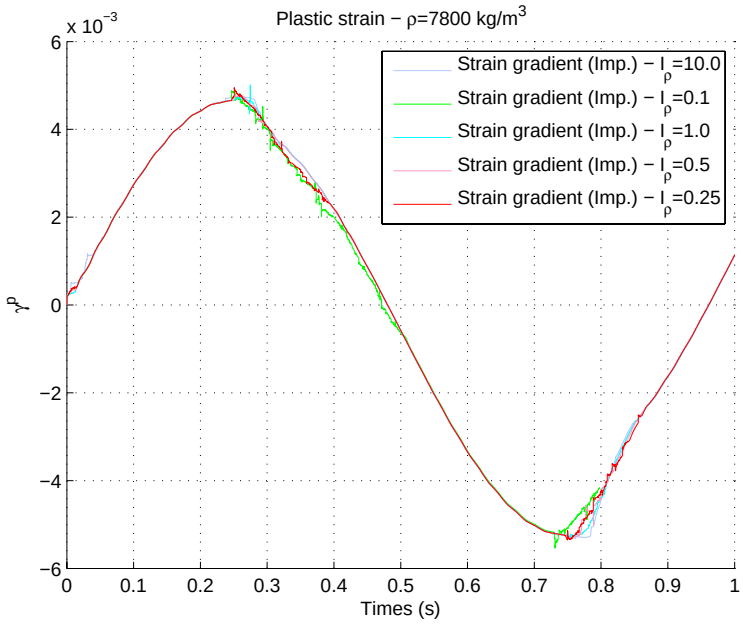

Figure16. Case 4 - Shear plastic strains γ^p at $y = 9.925m$

of shear plastic strain γ^p along the length of the rod, which are depicted in Figure 19, are nearly uniform as we expected for the case using the conventional plasticity theory.

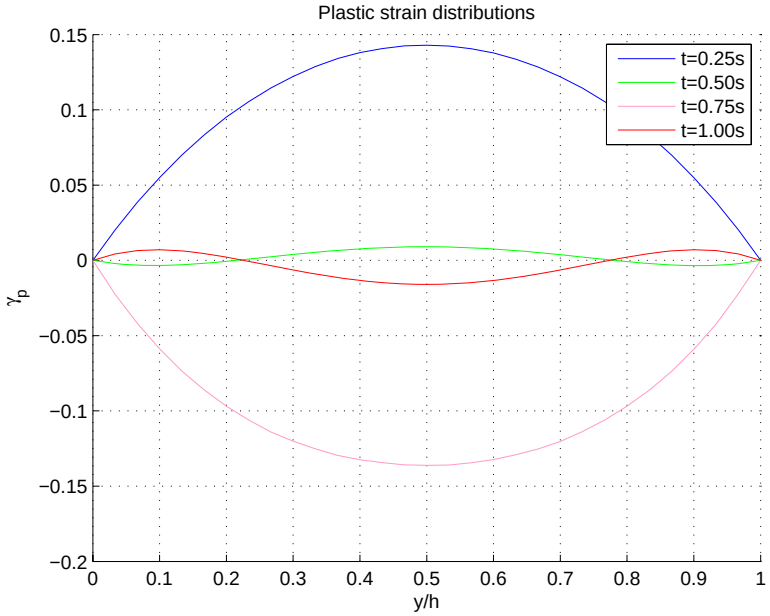

Figure17. Case 4 - Distribution of shear plastic strain γ^p, $I_\rho = 0.25\frac{kg}{m}$

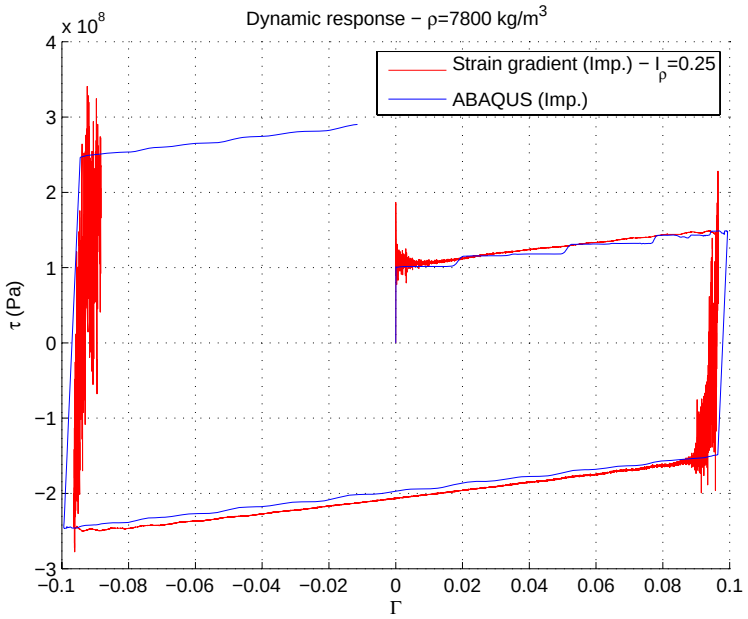

Figure18. Case 5 - Dynamic response $\Gamma - \tau$ at $y = 9.925m$

5 Conclusion

A one-dimensional dynamic analysis with the theory of strain-gradient viscoplasticity has been carried out. Several examples are presented and show how to simulate the dynamic effects of structures with viscoplastic material behavior. The plastic shear strain is chosen as indicator of microscopic defects in materials through length scale parameters in order

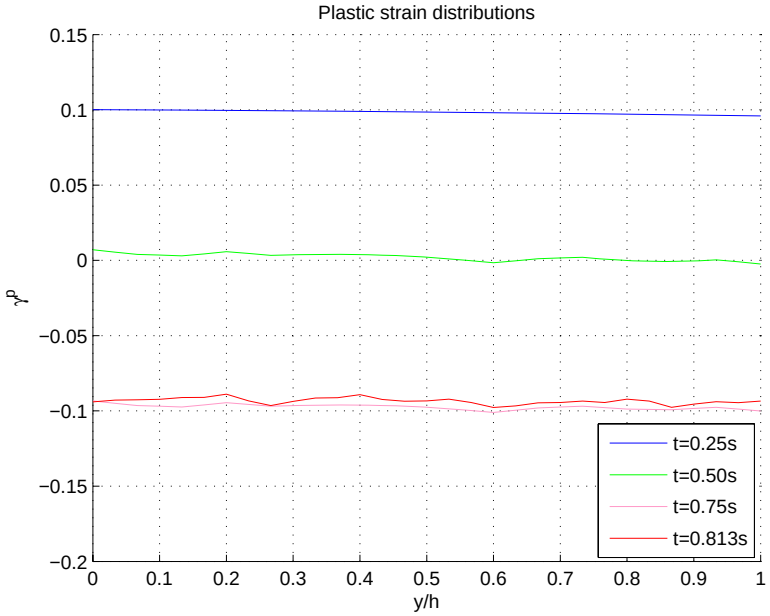

Figure19. Case 5 - Distribution of shear plastic strain γ^p, $I_\rho = 0.25\frac{kg}{m}$

to take into account the microscopic inertia effects. A parameter study of the microscopic inertia factor gives that the best value of microscopic-inertia parameter is $0.25\frac{kg}{m}$ being able to cover the conventional plasticity theory. For numerical aspects, first it is noted here that due to the extra requirements of boundary conditions on plastic strain rates at the free ends of the strip the distribution of plastic strain along the strip is not same as that obtained from conventional plasticity. Then, due to the expense of the loss of accuracy, small artificial damping occurs and introduces dynamic effects.

Appendix: Hilber-Hughes-Taylor's time integration scheme

Hilber-Hughes-Taylor's time integration scheme (ABAQUS, Hilber (1977), Hilber(1978)), which is used to obtain the approximate solutions by one step difference method, is briefly summarized here.

$$-\boldsymbol{M}\ddot{\boldsymbol{U}} + (1+\alpha)\boldsymbol{G}_{t+\Delta t} - \alpha\boldsymbol{G}_t = 0 \tag{32}$$

$$\boldsymbol{U}_{t+\Delta t} = \boldsymbol{U}_t + \Delta t\, \dot{\boldsymbol{U}}_t + \Delta t^2 \left[\left(\frac{1}{2} - \beta\right)\ddot{\boldsymbol{U}}_t + \beta\ddot{\boldsymbol{U}}_{t+\Delta t}\right] \tag{33}$$

$$\dot{\boldsymbol{U}}_{t+\Delta t} = \dot{\boldsymbol{U}}_t + \Delta t \left[(1-\gamma)\,\ddot{\boldsymbol{U}}_t + \gamma\ddot{\boldsymbol{U}}_{t+\Delta t}\right] \tag{34}$$

$$\boldsymbol{U}_0 = \bar{\boldsymbol{U}} \tag{35}$$

$$\dot{\boldsymbol{U}}_0 = \dot{\bar{\boldsymbol{U}}} \tag{36}$$

$$\ddot{\boldsymbol{U}}_0 = \boldsymbol{M}^{-1}\left(\boldsymbol{F}_0 - \boldsymbol{K}\boldsymbol{U}_0\right) \tag{37}$$

where β, γ are Newmark parameters (Newmark(1959)) of the integration scheme are defined by

$$\beta = \frac{1}{4}(1-\alpha)^2, \quad \gamma = \frac{1}{2} - \alpha \text{ and } -\frac{1}{3} \leq \alpha \leq 0 \tag{38}$$

The "static" force vector $\boldsymbol{G}$ is defined by

$$\boldsymbol{G}_{t+\Delta t} = \boldsymbol{P}_{t+\Delta t} - \boldsymbol{I}_{t+\Delta t} \tag{39}$$

$$\boldsymbol{G}_t = \boldsymbol{P}_t - \boldsymbol{I}_t \tag{40}$$

The residual force vector $\boldsymbol{F}$ is determined by

$$\boldsymbol{F} = -\boldsymbol{M}\ddot{\boldsymbol{U}} + (1+\alpha)\boldsymbol{G}_{t+\Delta t} - \alpha \boldsymbol{G}_t \tag{41}$$

The Jacobian matrix has the form

$$\boldsymbol{A} = -(1+\alpha)\frac{\partial \boldsymbol{F}}{\partial \boldsymbol{U}} - (1+\alpha)\frac{\partial \boldsymbol{F}}{\partial \dot{\boldsymbol{U}}}\left(\frac{d\dot{U}}{dU}\right)_{t+\Delta t} - \frac{\partial \boldsymbol{F}}{\partial \ddot{\boldsymbol{U}}}\left(\frac{d\ddot{U}}{dU}\right)_{t+\Delta t} \tag{42}$$

$$= \boldsymbol{K} + (1+\alpha)\boldsymbol{C}\left(\frac{d\dot{U}}{dU}\right)_{t+\Delta t} + (1+\alpha)\boldsymbol{M}\left(\frac{d\ddot{U}}{dU}\right)_{t+\Delta t} \tag{43}$$

where

$$\left(\frac{d\dot{U}}{dU}\right)_{t+\Delta t} = \frac{\gamma}{\beta \Delta t} \tag{44}$$

$$\left(\frac{d\ddot{U}}{dU}\right)_{t+\Delta t} = \frac{1}{\beta \Delta t^2} \tag{45}$$

For an accuracy of the solution and an approximate adjustment of the time step, half step residual is also needed

$$\boldsymbol{F} = -\boldsymbol{M}\ddot{\boldsymbol{U}}_{t+\Delta t/2} + (1+\alpha)G_{t+\Delta t/2} - \alpha\left(G_t + G_{t_-}\right) \tag{46}$$

References

1. ABAQUS Manuals v.6.8

2. Anand L., Gurtin M.E., Lele S.P., Gething C., 2005. A one-dimensional theory of strain-gradient plasticity: Formulation, analysis, numerical results. J. Mech. Phys. Solids Vol. **53**, 1789–1826.

3. Aifantis E. C., 1984. On the microstructural origin of certain inelastic models. J. Eng. Mat. Tech. **106**, 326-330.

4. Aifantis E.C., 1987. The physics of plastic deformation. Int. J. Plast. Vol. **3**, 211-247.

5. Aifantis E.C., 1992. On the role of gradients in localization of deformation and fracture. Int. J. Eng. **30**, No. **30**, 1279-1299.

6. Askes H., Pamin J., Borst R.D., 2000. Dispersion analysis and element-free Galerkin solutions of second- and fourth-order gradient-enhanced damage models. Int. J. Num. Meth. Eng. **49**, No. **6**, 811-832.

7. Borst R.D., Mülhhaus H.-B., 1992. Gradient-dependent plasticity: formulation and algorithmic aspects. Int. J. Num. Meth. Eng. **35**, 521-539.

8. Borst R.D., Pamin J., Peerlings R.H.J, Sluys L.J., 1995. On gradient-enhanced damage and plasticity models for failure in quasi-brittle and frictional materials. Comp. Mechanica **17**, 130-141.

9. Borst R.D., Pamin J., 1996. Some novel developments in finite element procedures for gradient-depdent plasticity. Int. J. Num. Meth. Eng. **39**, 2477-2505.

10. Borst R.D., Pamin J., Geers M.G.D., 1999. On coupled gradient-dependent plasticity and damage theories with a view to localization analysis. Eur. J. Mech. A.Solids **18**, 939-962.

11. Fleck N.A., Hutchinson J.W., 1993. A phenomenological theory for strain gradient effects in plasticity. J. Mech. Phys. Sol. **41**, 12, 1825-1857.

12. Fleck N.A., Muller G.M., Ashby M.F., Hutchinson J.W., 1994. Strain gradient plasticity: theory and experiment. Acta Met. Mat. (UK) **42**, 2, 475-487.

13. Fleck N.A., Hutchinson J.W., 2001. A reformulation of strain gradient plasticity. J. Mech. Phys. Sol. **49**, 2245-2271.

14. Forest S., Sievert R., 2001. Elastoviscoplastic constitutive frameworks for generalized continua. Acta Mech. **160**, 71-111.

15. Gudmundson P., 2004. A unified treatment of strain gradient plasticity. J. Mech. and Phys. Sol. **52**, 1379-1406.

16. Gurtin M.E., 2000. On the plasticity of single crystals: free energy, microforces, plastic-strain gradients. J. Mech. Phys. Sol. **48**, 989-1036.

17. Gurtin M.E., 2002. A gradient theory of single-crystal viscoplasticity that accounts for geometrically necessary dislocations. J. Mech. Phys. Sol. **50**, 5-32.

18. Gurtin M.E., 2003. On a framework for small-deformation viscoplasticity: free energy, microforces, strain gradients. Int. J. Plast. 19, 47-90.

19. Hilber H.M., Hughes T.J.R., Taylor R.L., 1977. Improved numerical disspation for time integration algorithms in structural dynamics. Earth. Eng. Struct. Dyn. **5**, 283-292.

20. Hilber H.M., Hughes T.J.R., 1977. Collocation, dissipation and 'overshot' for time integration schemes in structural dynamics. Earth. Eng. Struct. Dyn. **6**, 99-117.

21. Lele S.P., 2008. On a class of strain gradient plasticity theories: formulation and numerical implementation. Dissertation, Massachusetts Institute of Technology, USA.

22. Lele S.P., Anand L., 2008. A small-deformation strain-gradient theory for isotropic viscoplastic materials. Phil. Mag. **88**, No.30-32, 3655-3689.

23. Lele S.P., Anand L., 2009. A large-deformation strain-gradient theory for isotropic viscoplastic materials. Int. J. Plast. **25**, pp. 420-453 (2009).

24. Luzio G.D., Bazant Z.D., 2005. Spectral analysis of localization in nonlocal and over-nonlocal materials with softening plasticity or damage. Int. J. Sol. Struct. **42**, 6072-6100.

25. Kong S., Zhou S., Nie Z., Wang K., 2009. Static and dynamic analysis of micro beams based on strain gradient elasticity theory. Int. J. Eng. Sci. **47**, 487-498.

26. Newmark N.M., 1959. A method of computation for structural dynamics. J. Eng. Mech. Div., Proceedings of ASCE **85**, 67-94.

27. Makowski J., Stumpf H., Hackl K., 2006. The fundamental role of nonlocal and local balance laws of material forces in finite elastoplasticity and damage mechanics. Int. J. Sol. Struct. **43**, 3940-3959.

28. Metrikine A.V., Askes H., 2002a. One-dimensional dynamically consistent gradient elasticity models derived from a discrete microstructure Part 1: Generic formulation. Eur. J. Mech. A/Solids **21**, 555-572.

29. Metrikine A.V., Askes H., 2002b. One-dimensional dynamically consistent gradient elasticity models derived from a discrete microstructure Part 2: Static and dynamic response. Eur. J. Mech. A/Solids **21**, 573-588.

30. Mühlhaus H.-B., Aifantis E.C., 1992. A variational principle for gradient plasticity. International Journal of Solids and Structures **28** (7), 845-847.

31. Peerlings R.H.J., de Borst R., Brekelmans W.A.M., Spee I., 1996. Some observations on localisation in non-local and gradient damage models. Eur. J. Mech. A/Solids **15** (6), 937-953.

32. Peerlings R.H.J., de Borst R., Brekelmans W.A.M., Geers M.G.D., 1998. Wave propagation and localisation in nonlocal and gradient-enhanced damage models. J. de Phys. IV **8**, 293-300.

33. Peerlings R.H.J., Geers M.G.D., Borst R.D., Brekelmans W.A.M., 2001. A critical comparision of nonlocal and gradient-enhanced softening continua. International Journal of solidas and Structures **38**, 7723-7746.

34. Sluys L.J., 1996. Wave propagation, localization and dispersion in softening solids. Dissertation, Delft University of Technology, Delft.

35. Sluys L.J., Cauvern M., Borst R.D., 1995. Discretization influence in strain-softening problems. Eng. Comp. **12**, 209-228.

36. Nguyen Q.S., Andrieux S., 2005. The non-local generalzed standard approach: a consistent gradient theory. Comptes Rendus Mecanique **333**, 139-145.

37. Voyiadjis G.Z., Abu Al-Rub R.K., Palazotto A.N., 2004. Thermodynamic framework for coupling of non-local viscoplasticity and non-local anisotropic viscodamage for dynamic localization problems using gradient theory. Int. J. Plast. **20**, 981-1038.

38. Zbib H.M., Aifantis E.C., 1989. A Gradient-Dependent Flow Theory of Plasticity: Application to Metal and Soil Instabilities. Appl. Mech. Rev. **42** (11), 295-304.

39. Pamin J.K., 1994. Gradient-Dependent Plasticity in Numerical Simulation of Localization Phenomena. Dissertation, University Press, TU Delft.